Technical Note

Real time forecast service for geomagnetically induced currents

WP 300
Computation of GIC from the geomagnetic field

Ari Viljanen, Risto Pirjola and Antti Pulkkinen*
Finnish Meteorological Institute
Space Research Unit
P.O.B. 503, FIN-00101 Helsinki, Finland

September 17, 2004

*Now at NASA/GSFC

Document status sheet

Document title: Technical Note, Real time forecast service for geomagnetically induced currents, WP 300: Computation of GIC from the geomagnetic field

Issue: 0.0

Revision: 0

Document change record:

Autumn 2004: First draft (0.0)

Abstract

TO BE WRITTEN.

Contents

1 Introduction

The Space Research Unit of the Finnish Meteorological Institute is involved in three service development activities (SDA) within the ESA Space Weather Pilot Programme:

- Auroras Now! and GIC Now! (PI: FMI)
- Real Time Forecast Service for Geomagnetically Induced Currents (PI: IRF-Lund, Sweden)
- Real-Time GIC Simulator (PI: GSC, Canada)

WP 300 of "Real Time Forecast Service for Geomagnetically Induced Currents" deals with the calculation of GIC in a power system. This technical note describes the methods and software used for that purpose.

1.1 Definitions, acronyms and abbreviations

ESTEC = European Space Research and Technology Centre
FFT = Fast Fourier Transform
FMI = Finnish Meteorological Institute
GIC = geomagnetically induced current
IMAGE = International Monitor for Auroral Geomagnetic Effects, a magnetometer network in northern Europe (http://www.geo.fmi.fi/image/)
SDA = service development activity
WP = work package
WWW = World Wide Web

$\mathbf{E} = E_x\mathbf{e}_x + E_y\mathbf{e}_y$ = horizontal electric field vector (x to the geographic north, y to the east)
$\mathbf{H} = B_x\mathbf{e}_x + B_y\mathbf{e}_y$ = horizontal magnetic field vector
$d\mathbf{H}/dt$ = time derivative of $\mathbf{H}$

2 Calculation of the geoelectric field

2.1 Calculation of the geoelectric field

The simplest way to determine the geoelectric field from geomagnetic recordings is to apply the local plane wave model (Viljanen et al., 2004). This means that the surface electric field is related to the local geomagnetic field by the surface impedance $Z(\omega)$:

$$E_x(\omega) = Z(\omega)B_y(\omega)/\mu_0,\ E_y(\omega) = -Z(\omega)B_x(\omega)/\mu_0 \tag{1}$$

where ω is the angular frequency and μ_0 is the vacuum permeability. The time-domain values are obtained by the Fourier transform (FFT in computer executions). With a special case of a uniform earth with conductivity σ, the time-domain formula is simple:

$$E_x(t) = \frac{1}{\sqrt{\pi\mu_0\sigma}}\int_{-\infty}^{t}\frac{g_y(u)}{\sqrt{t-u}},\ E_y(t) = -\frac{1}{\sqrt{\pi\mu_0\sigma}}\int_{-\infty}^{t}\frac{g_x(u)}{\sqrt{t-u}} \tag{2}$$

where $g(t) = dB(t)/dt$ is the time derivative of the magnetic field. These expressions show explicitly that the electric field depends on all previous values of the magnetic field, although the most recent ones have the largest effect. It is also obvious that dB/dt is a reasonable indicator of GIC activity.

The surface impedance depends on the local 1-D conductivity structure of the earth. We assume here that the same model can be used in whole study region. However, it is also possible to refine the method by selecting different 1-D models for different sites. As a starting point of earth models, we can use the results by Korja et al. (2002) which indicate typical values in the Fennoscandian Shield. A quantitative fitting of the local conductivity model requires measured GIC values.

The magnetic field is recorded continuously at several sites in northern Europe (Fig. 1). The most convenient way to provide the electric field input to GIC programs is to use a regular grid covering the power system studied. So the first step is to interpolate the magnetic field at the same grid (Fig. 2). This is described in the technical note of WP 200.

We have used here a much wider magnetometer network than would be necessary for studies in southern Sweden. However, the database is now readily available for possible later extensions to other parts of Sweden or neighbouring countries. Furthermore, the same data are useful for scientific investigations too.

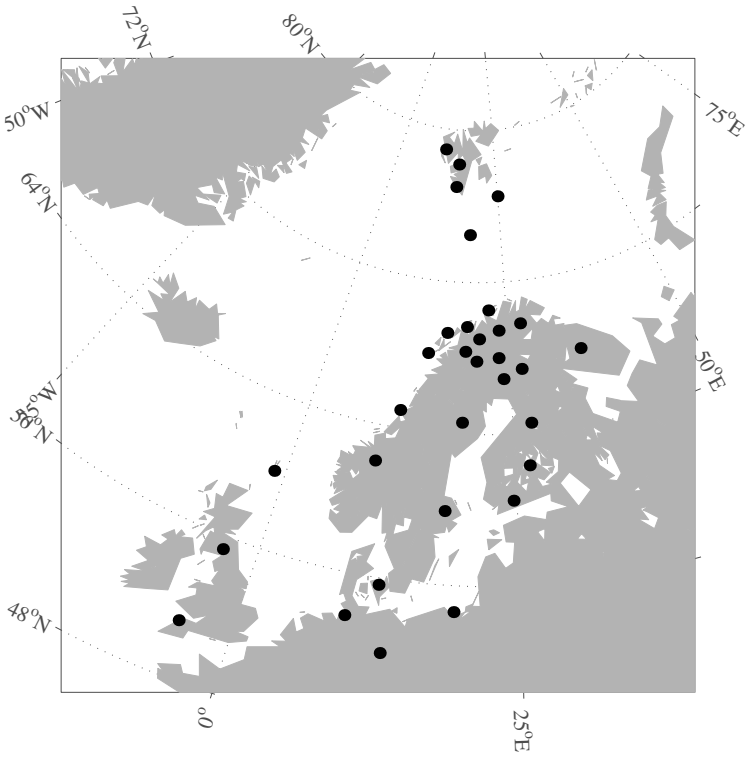

Figure 1: Magnetometer stations used for the magnetic field interpolation in southern Sweden.

In the practical computation, we take a finite sample of the magnetic field time series. We apply a window function to the data to force the first and last values of the sample to be equal to reduce Gibb's phenomenon always related to Fourier series. We have used the Parzen window:

$$W = 1 - [\frac{2(n - N/2)}{N}]^8 \tag{3}$$

for $n = 1, ..., N$ and $W = 0$ otherwise.

2.2 Validation of the plane wave method

It is possible to use a different conductivity model for each grid point. However, when a relatively small region like southern Sweden is considered, it is

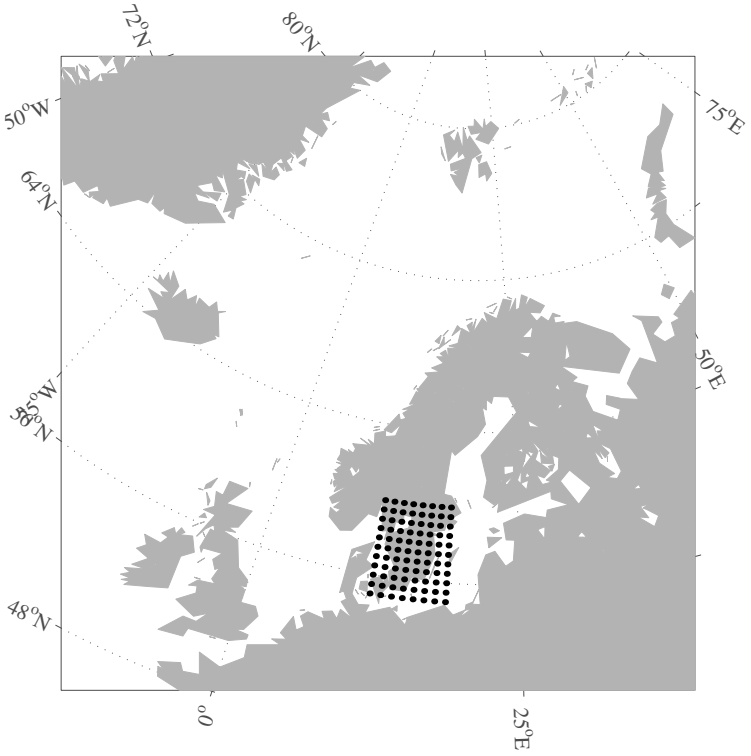

Figure 2: The dense grid covering southern Sweden.

more appropriate to assume the same earth model for the whole area. This approach has been successfull also in Finland with power system studies and with pipeline studies (Viljanen et al., 2004; see also the GIC Now! SDA technical note).

It is even reasonable to use the magnetic field of a single site to calculate the electric field on the whole study region. We have applied this in GIC Now! where we use real-time data from the Nurmijärvi geophysical observatory to calculate the electric field in the area of the whole Finnish natural gas pipeline. The electric field is generally not spatially constant at such a large region, so a single-point magnetic field measurement may not sound sufficient. However, Viljanen et al. (2004) showed that in southern Finland the geoelectric field is spatially quite uniform in the east-west direction in an area of a 100-200 km length scale. So the electric field calculated at

Nurmijärvi provides a reasonable proxy. We can safely assume that the situation is equally favourable in southern Sweden, and we will also demonstrate this explicitly below.

Examples of the input magnetic field (horizontal component $\mathbf{H}$), its time derivative and the calculated electric field are shown in Figs. 3-5. The event is selected during a period with large $d\mathbf{H}/dt$ values on the region. A typical feature is that the magnetic field is spatially very uniform, whereas $d\mathbf{H}/dt$ is more structured. This is related to small-scale ionospheric currents with a relatively uniform main flow in background (Pulkkinen et al., 2003). The pattern of the horizontal electric field is roughly obtained from $d\mathbf{H}/dt$ by a 90 degrees anticlockwise rotation. However, this is not a one-to-one relationship, but the history of $d\mathbf{H}/dt$ affects the detailed structure (Eq. 2). In other words, the earth affects as a filter smoothing the most rapid temporal variations of $d\mathbf{H}/dt$.

To measure the spatial uniformity of the field, we calculate the difference of $\mathbf{H}$ between each pair of sites and compare it to the sum of magnitudes of $\mathbf{H}$:

$$u(t) = 1 - \frac{2}{N(N-1)} \sum_{m=1}^{N} \sum_{n=m+1}^{N} \frac{|\mathbf{H}_m(t) - \mathbf{H}_n(t)|}{|\mathbf{H}_m(t)| + |\mathbf{H}_n(t)|} \tag{4}$$

where $\mathbf{H}_m(t)$ is given at site m at time t and N is the total number of sites. If the field is completely uniform then $u = 1$. Note that with the normalization used in Eq. 4 u can vary only between 0 and 1, because $0 \leq |\mathbf{a}-\mathbf{b}| \leq |\mathbf{a}|+|\mathbf{b}|$, when the double sum is at most $N(N-1)/2$.

Uniformity indicators during one day are shown in Figs. 6-8 using the same definition for $\mathbf{H}$, $d\mathbf{H}/dt$ and $\mathbf{E}$. Visual inspection shows that, despite its simplicity, u is a reasonable indicator. Statistical results are presented in Figs. 9-11. Both single day results and statistical results show that $\mathbf{H}$ is quite smooth whereas $d\mathbf{H}/dt$ and $\mathbf{E}$ are more variable. Statistical results show that $\mathbf{E}$ is also spatially slightly more uniform than $d\mathbf{H}/dt$. There is no obvious correlation between the amplitude of the field and the spatial uniformity (Figs. 6-8).

Although these results indicate that the electric field is spatially a little smoother than the time derivative of the magnetic field, a careful interpretation is necessary. First of all, we have assumed the same conductivity model throughout the region. Although in a large scale this seems to be a good assumption in southern Sweden (Korja et al., 2002, Fig. 9), there are always very small-scale anomalies. It follows that a pointwise measured electric

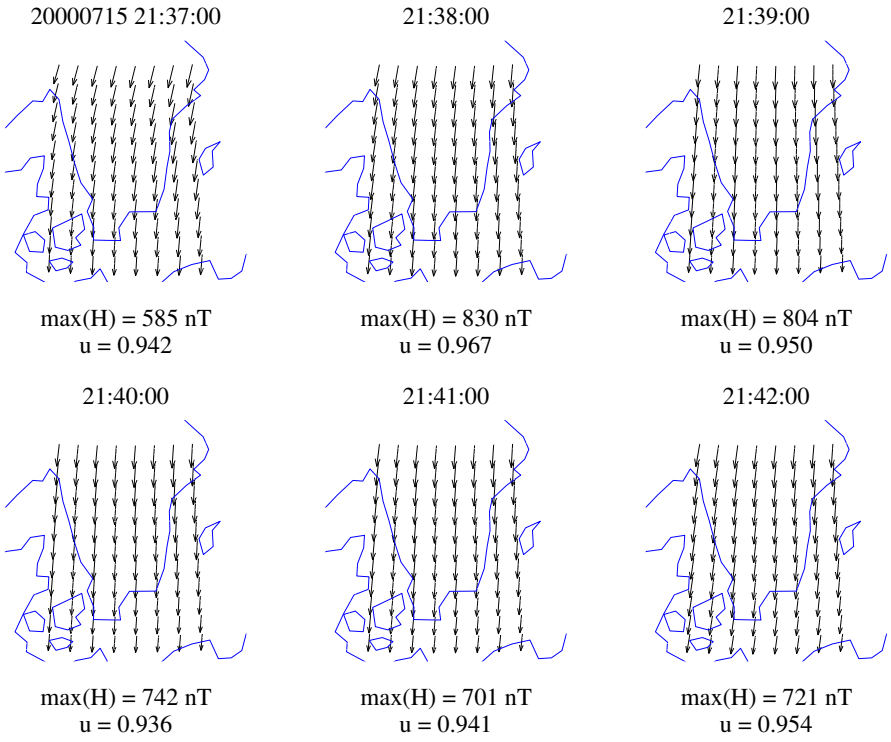

Figure 3: Snapshots of interpolated horizontal magnetic field vectors. The uniformity of the field is given by the quantity u (Eq. 4).

field has a rapid spatial variation (even in the scale of one km), whereas the magnetic field is less affected. The physical reason is that lateral conductivity anomalies cause charge accumulation, so the electric field is affected both by charges and currents; the magnetic field is only caused by currents. The model calculations above assume a layered earth, when there is no charge accumulation at all. In other words, these calculations show that the nonuniformity of the electric field due to spatially varying ionospheric currents is not very large in this region.

A natural question is whether simple layered earth models are adequate. This seems to be the case, because GIC at a given site is not related to the local electric field at the same site, but to the regional average. GIC is driven by voltages integrated from the electric field along power lines. Integration is

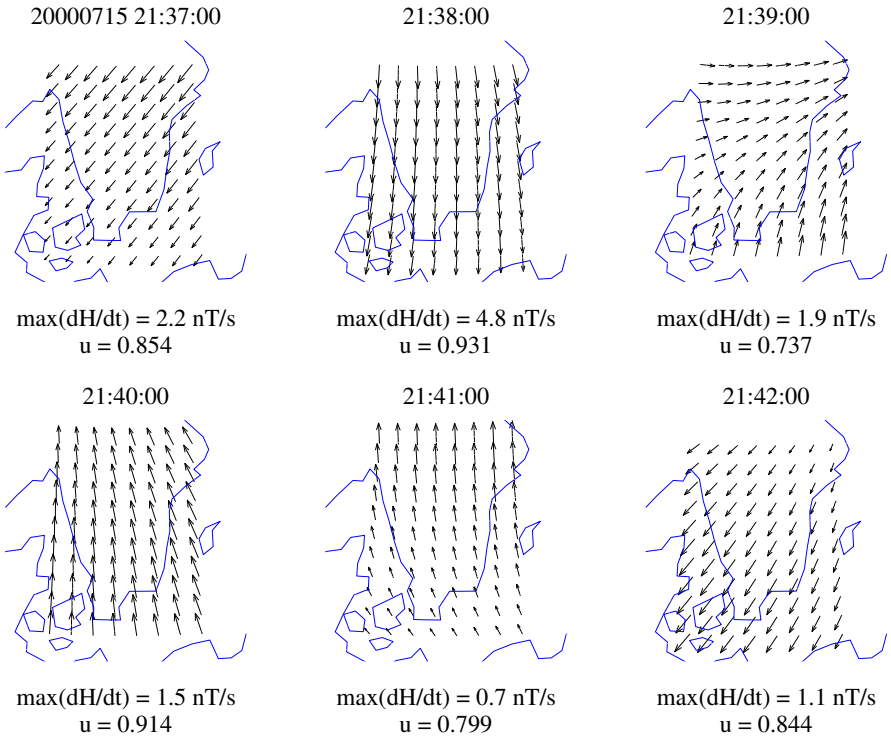

Figure 4: As Fig. 3, but for the interpolated time derivative of horizontal magnetic field vectors.

a spatially smoothing operation, so small-scale anomalies are not significant. Furthermore, when a given site is considered then it is not necessary to know the electric field at distant regions, but the area defined by the nearest earthing points is dominating. Experiences in modelling GIC in the Finnish power system and natural gas pipeline support these conclusions (Viljanen et al., 2004).

2.3 Calculation of GIC from the electric field

The conventional way has been to divide GIC modelling into two independent parts:
1. Determination of the geoelectric field.

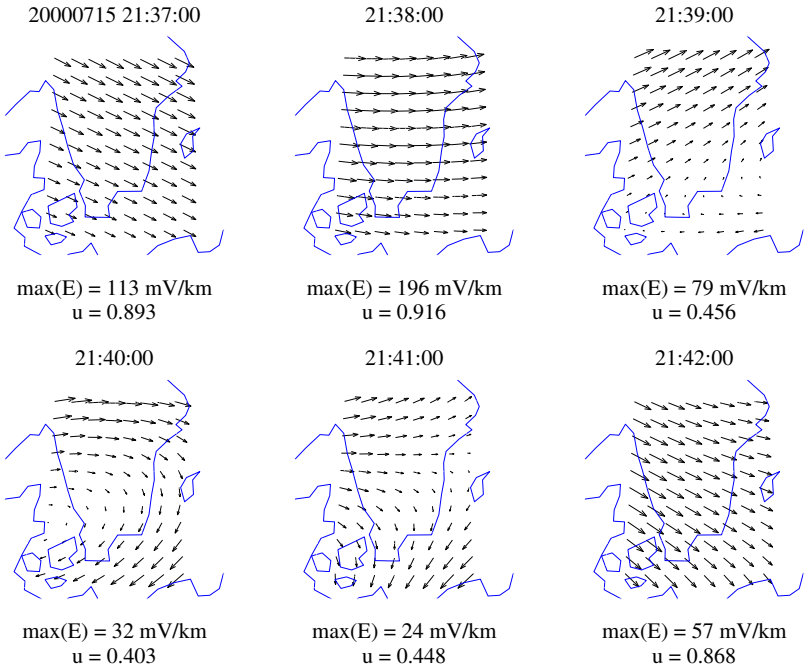

Figure 5: As Fig. 3, but for the calculated geoeletric field.

2. Calculation of GIC using the given geoelectric field.
The first step assumes implicitly that the power system has no effect on the electric field. This is a reasonable approximation as known from experience. A recent rigorous theoretical discussion also supports this (Pulkkinen, 2003).

The second step requires that the electromagnetic parameters and the geometry of the power system are known. Because GIC is a low-frequency phenomenon (compared to the 50 Hz AC frequency), a DC model is sufficient (Pulkkinen, 2003). The basic modelling technique applied here is presented by Lehtinen and Pirjola (1985).

It follows from the assumption of a spatially uniform electric field that GIC at a given site is

$$GIC(t) = aE_x(t) + bE_y(t) \tag{5}$$

where E_x, E_y are the north and east components of the electric field. The coefficients a, b depend only on the geometry and resistances of the power

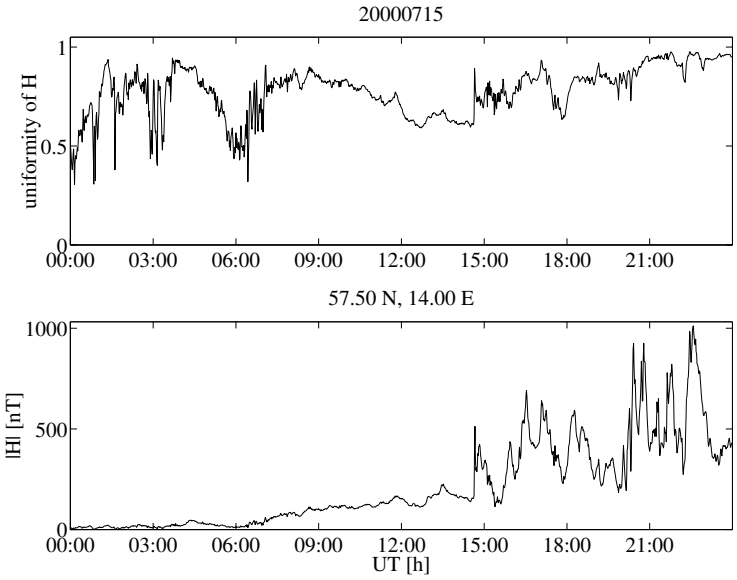

Figure 6: Upper panel: Uniformity of the interpolated horizontal magnetic field on July 15, 2000, in the dense grid of Fig. 2. Lower panel: Magnitude of the horizontal field in the centre of the grid.

system. So for a fixed network, these coefficients must be determined only once, which makes computations very fast. If the electric field varies spatially then it must be integrated along power lines separately for each timestep.

Equation 5 also allows a straighforward determination of GIC without an explicit power system model. Then we need the electric field at a nearby location to the GIC site, and measured GIC values. It is also necessary to assume that the configuration of the power grid does not change during the period studied. We applied this approach to the GIC data at a Swedish transformer in 1998-2000, and fitted the coeffiecients a and b in Eq. 5 minimising the difference between modelled and measured GIC. We used the modelled geoelectric field at the point 57 N, 16 E. Because large GIC values are most important, we considered only timesteps with $|GIC| > 10$ A in the fitting. Furthermore, the accuracy of GIC data is only 1 A, so it is not meaningful to use GIC values of only a few amperes. The empirical relation between GIC and the electric field is

$$GIC(t) = 0.1604E_x(t) - 0.6865E_y(t) \tag{6}$$

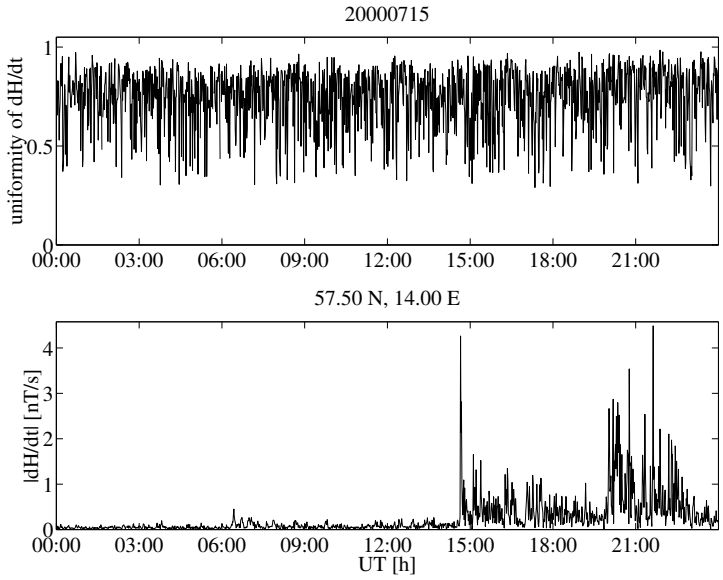

Figure 7: Upper panel: Uniformity of the interpolated time derivative of the horizontal magnetic field on July 15, 2000, in the dense grid of Fig. 2. Lower panel: Magnitude of the time derivative of the horizontal field in the centre of the grid.

The electric field is given in mV/km and GIC is obtained in amperes. This formula is approximately valid in the period Sep 1998 - Oct 2000. The result shows that GIC at this site was mainly determined by the eastward component of the electric field.

The measured GIC time series was shifted two minutes backwards due to an obvious timing error. This shift provided the smallest fitting error and also yielded the best visual correspondence of modelled and measured GIC curves.

The median model error for $|GIC| > 10$ A was 10.3 A, which is quite large. This may be due to occasional changes in the power grid near the GIC site, or due to measurement problems. The event-to-event variability is quite large as shown in Fig. 12. However, when large number of GIC values were available, the single event multipliers a and b are close to the "global" value. A clear exception is the big storm of April 6, 2000, when the modelled values are much smaller than the measured ones. We also studied the effect

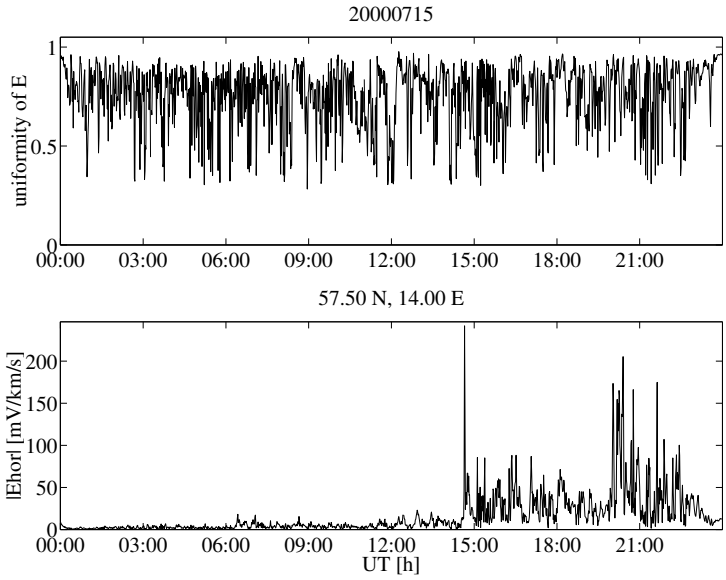

Figure 8: Upper panel: Uniformity of the calculated geoeletric field on July 15, 2000, in the dense grid of Fig. 2. Lower panel: Magnitude of the horizontal electric field in the centre of the grid.

of different GIC limits on the coefficients a and b and on the fitting error. Results are shown in Table 1. It is clear that the empirical fitting is not an optimal solution in this case.

Table 1: Coefficients a and b (Eq. 5) with different limits of large GIC values used in the fit.

limit [A]	#	a	b	median error [A]	rel. error [%]
5	3387	0.0644	-0.6122	5.7	69
10	1498	0.1604	-0.6865	10.3	67
15	845	0.2862	-0.7608	13.7	63
20	556	0.3359	-0.8210	17.9	62
30	271	0.5738	-0.9326	23.4	58

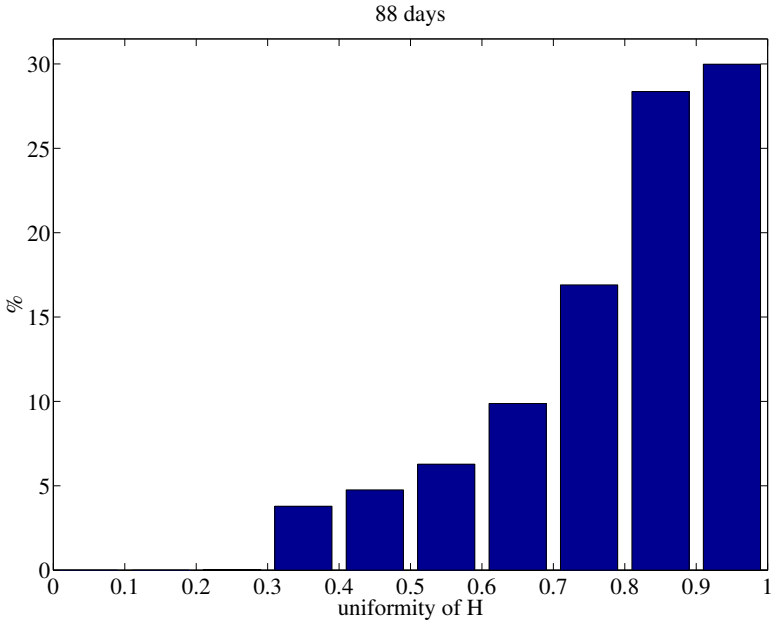

Figure 9: Uniformity of the interpolated horizontal magnetic field during the selected days.

2.4 Full network modelling

TO BE DONE.

3 GIC software

3.1 General

TO BE WRITTEN.

3.2 Data formats

The interpolated magnetic field is stored in MatLab binary files named as interpBYYYYMMDD.mat (YYYYMMDD = year, month, day). It contains the following variables:

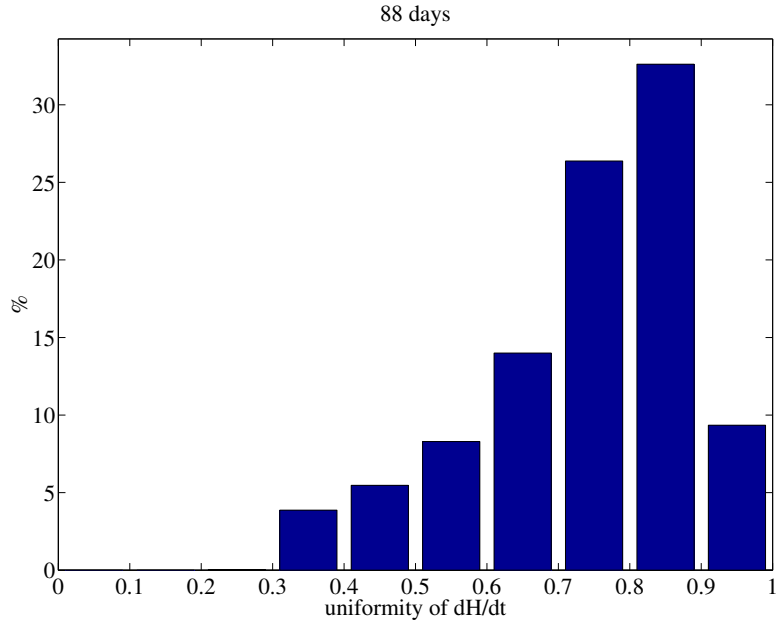

Figure 10: Uniformity of the interpolated time derivative of the horizontal magnetic field during the selected days.

BX, BY, BZ: geographic north, east and downwards components of the magnetic field (NxM matrices, each row corresponding to one timestep and each column corresponding to one site)
$Bunit$: scaling factor with which the magnetic field must be multiplied to get it in nT (scalar)
$year, month, day$: day of the event (scalars)
t: UT in decimal hours (vector of length N)
$interval$: time step in seconds between successive observations (scalar)
$lat, long$: geographic latitudes and longitudes of the surface grid points (vectors of length M)
$names$: names of the grid point "stations" (string array with M rows)

Some variables (baseline, baselinestring) are not needed here, but the binary file is intentionally in the format used at FMI in other studies. Quiet time baselines are subtracted from the data used in this study. Baselines are selected visually for each event. This is a satisfactory method, since concerning

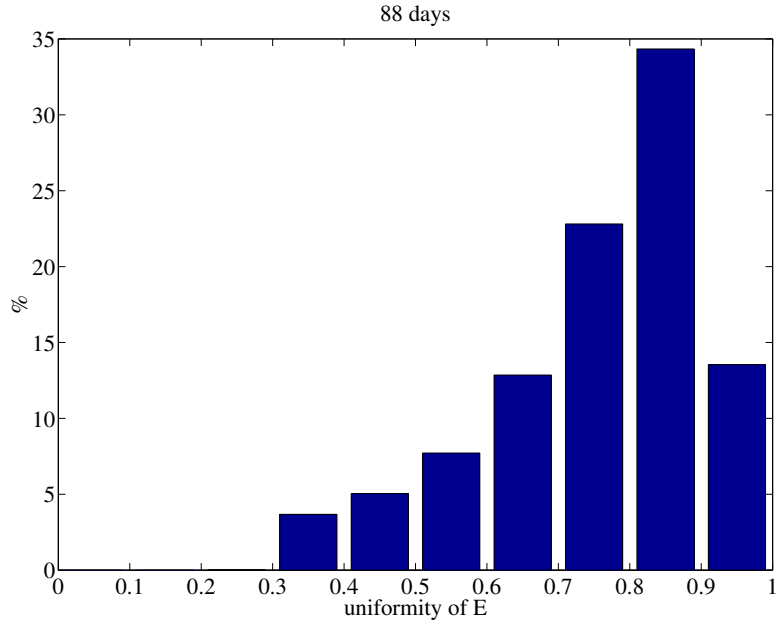

Figure 11: Uniformity of the calculated geoeletric field during the selected days.

large variations, the exact selection criteria for a quiet time are not critical.

The calculated electric field is also saved as MatLab binary files named as exey_irf_YYYYMMDD.mat, and containing the following variables:

EX, EY: geographic north and east components of the electric field (NxM matrices, each row corresponding to one timestep and each column corresponding to one site)
$Bunit$: scaling factor with which the electric field must be multiplied to get it in mV/km (scalar)
$year, month, day$: day of the event (scalars)
t: UT in decimal hours (vector of length N)
T: time step in seconds between successive observations (scalar)
$lat, long$: geographic latitudes and longitudes of the surface grid points (vectors of length M)
$mywindow$: window function multiplying the input magnetic field time series

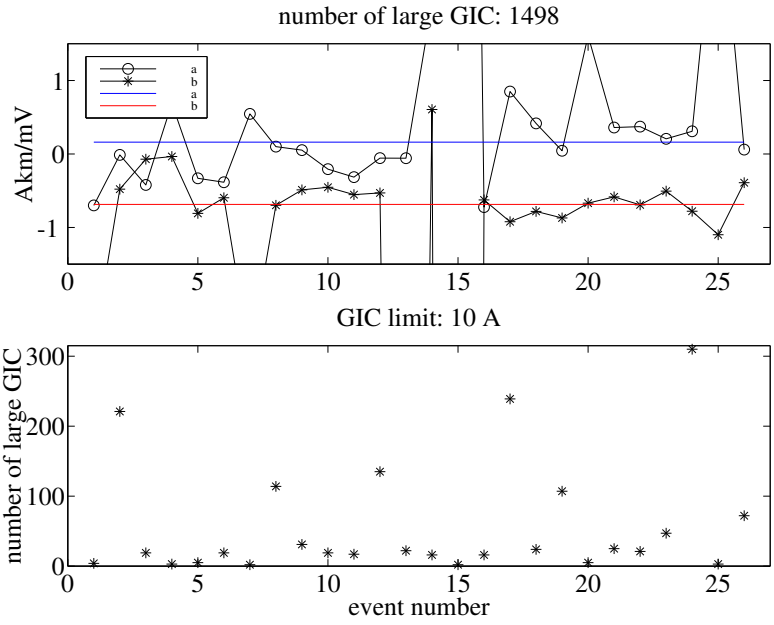

Figure 12: The upper panel shows the event-to-event variability of the multipliers a (circle) and b (asterisk) in Eq. 5. The "global" values in Eq. 6 are shown as blue (a) and red (b) lines. The number of large GIC values used in each event is shown in the lower panel.

(vector of length N)
thick: thicknesses of the earth layers [m]; note that the lowest layer has an infinite depth and is not included in this vector of length $P-1$
sigma: conductivities of the earth layers in 1/ohmm (vector of length P)
myy: permeabilities of the earth layers in SI units (vector of length P); reasonable values are equal to the vacuum permeability
epsilon: permittivities of the earth layers in SI units (vector of length P); due to the insignificance of the displacement current in the earth, exact values are not needed

Measured GIC are given in a single ASCII file with each line containing the following data values: year month day hour minute second GIC. Time is given in UT and GIC in amperes. The same data are also available as a single MatLab binary file containing one data matrix with the same format as given above.

3.3 List of MatLab files

- exey_irf.m
  The main routine to calculate the electric field from the interpolated magnetic field of the selected set of events.

- exey_calc_irf.m
  Subroutine for exey_irf.m to calculate the surface impedance and the electric field.

- plot_irf.m
  Plotting routine for the magnetic and electric fields of a single day.

- bxby_stat_irf.m
  Routine for a statistical analysis of the interpolated magnetic field of the selected set of events.

- exey_stat_irf.m
  Routine for a statistical analysis of the calculated magnetic field of the selected set of events.

- plot_gicdata_irf.m
  Simple plotting routine for the measured GIC. The program has also an option to save plots as eps files and to write automatically a LaTeX file containing these figures.

- fit_gicexey_irf.m
  Routine for fitting coefficients α and β in Eq. 5. The electric field calculated by exey_irf.m and the measured GIC data are needed as input. The program has also an option to save plots of measured and modelled GIC as eps files and to write automatically a LaTeX file containing these figures.

Calculation of the electric field for one day (1440 one-minute values) at 88 sites takes a few seconds on a Macintosh PowerBook G4 with a 867 MHz processor. Statistical analysis of the fields (of 27 days) takes a few minutes.

3.4 Conditions of use

To be defined in more details later.

All routines described in this document are directly based on pre-existing FMI software, which is considered as background information to all SDA's contributed by FMI. Delivery of the software package to a third party is allowed only in agreement with FMI.

4 Conclusions

TO BE WRITTEN.

Acknowledgements

FMI contribution to this SDA is to a great extent based on experiences obtained in Finland. Fingrid Oyj has contributed to studies on geomagnetically induced currents in the Finnish high voltage power system for nearly 30 years. Especially, we would like to thank Mr. Jarmo Elovaara and Mr. Matti Lahtinen for their continuous interest in our work.

5 References

Korja, T., M. Engels, A.A. Zhamaletdinov, A.A. Kovtun, N.A. Palshin, M.Yu. Smirnov, A.D. Tokarev, V.E. Asming, L.L. Vanyan, I.L. Vardaniants, and the BEAR Working Group, Crustal conductivity in Fennoscandia - a compilation of a database on crustal conductance in the Fennoscandian Shield, *Earth Planets Space*, **54**, 535–558, 2002.

Lehtinen, M. and R. Pirjola, Currents produced in earthed conductor networks by geomagnetically-induced electric fields. *Ann. Geophys.*, **3**, 479–484, 1985.

Pulkkinen, A., Geomagnetic induction during highly disturbed space weather conditions: Studies of ground effects. *Finnish Meteorological Institute Contributions*, **42**, 164 p., 2003.

Pulkkinen, A., A. Thomson, E. Clarke, and A. McKay, April 2000 geomagnetic storm: ionospheric drivers of large geomagnetically induced currents. *Ann. Geophys.*, **21**, 709–717, 2003.

Viljanen, A. and R. Pirjola, Statistics on geomagnetically-induced currents in the Finnish 400 kV power system based on recordings of geomagnetic variations. *J. Geomag. Geoelectr.*, **41**, 411–420, 1989.

Viljanen, A., A. Pulkkinen, O. Amm, R. Pirjola, T. Korja and BEAR Working Group, Fast computation of the geoelectric field using the method of elementary current systems and planar Earth models. *Ann. Geophys.*, **22**, 101–113, 2004.

A Appendix: Tests of GIC software

(Concerning operative executions.)

A.0.1 Normal operation

TO BE WRITTEN.

A.0.2 Simulated error cases

TO BE WRITTEN.

A.0.3 Error cases not simulated

TO BE WRITTEN.